Journal of Catalysis **198,** 172–178 (2001)
doi:10.1006/jcat.2000.3091, available online at http://www.idealibrary.com on IDEAL®

Photocatalytic Degradation of 1,3-Dihydroxy-5-methoxybenzene in Aqueous Suspensions of TiO_2: An Initial Kinetic Study

A. Neren Okte, Marianne Sowa Resat,[1] and Yüksel Inel[2]

Department of Chemistry, Bogazici University, Bebek/Istanbul, 80815 Turkey

Received March 13, 2000; revised October 4, 2000; accepted October 17, 2000; published online February 15, 2001

Photocatalytic degradation of 1,3-dihydroxy-5-methoxybenzene (1,3-DHMB) is investigated in the presence of TiO_2. Effects of initial concentration of 1,3-DHMB, pH of the medium, irradiation time, and temperature are examined. Degradation of 1,3-DHMB obeys zero-order kinetics. Following the formation of CO_2, the reaction rate constant, k, is found as 217 μmol m^{-3} s^{-1} and the adsorption constant, K, is found as 4.22 m^3 mol^{-1}. The highest degradation of 1,3-DHMB and the highest concentration of CO_2 are both obtained at pH 9.0. The apparent activation energy is calculated as 17.1 kJ/mol. For the route of degradation, a mechanism is postulated.

Key Words: **photocatalytic degradation; titanium dioxide; kinetics; degradation mechanism; 1,3-dihydroxy-5-methoxybenzene.**

1. INTRODUCTION

Degradation of organics (phenols, chlorophenols) by irradiating their aqueous titanium dioxide suspensions is of increasing technological and scientific interest over the past decade. Okamoto *et al.* (1) studied the effects of several parameters, such as, pH, O_2 partial pressure, initial phenol concentration, concentration of TiO_2, incident light intensity, and temperature on the reaction rate of phenol degradation. Results indicated that the photocatalytic decomposition of phenol over anatase TiO_2 powder followed first-order kinetics, up to high conversions, the apparent rate constant of which depended on the initial concentration of phenol, concentration of TiO_2, light intensity, and O_2 partial pressure. The activation energy was found to be 10 kJ/mol. Matthews and McEvoy (2) showed that the disappearance of phenol and the formation of CO_2 obey Langmuir-Hishelwood kinetics. The solution pH between 3.5 and 8.5 did not have a great effect on the degradation rates and the adsorption equilibrium constant was found to be dependent on the reciprocal of the initial phenol concentration. Wei and Wan (3) studied factors that influence the photocatalytic oxidation of phenol in oxygenated solution with suspensions of titanium dioxide powders. The pseudo-first-order reaction rate constant was found to be inversely proportional to the initial concentration of phenol. When pH effect was analysed, the competitive adsorption between phenoxide ions and OH^- ions on the TiO_2 surface was explained. Trillas *et al.* (4) reported that the yield of the phenol photooxidation depends strongly on the pH of the solution. Maximum yields were obtained at pH 8 and also in very alkaline media. Al-Sayyed *et al.* (5) determined the kinetics of disappearance of 4-chlorophenol in the presence of TiO_2 in water under illumination at $\lambda \geq 340$ nm and 293 K. The rate of disappearance of 4-chlorophenol is found to be increased upon increasing 4-chlorophenol concentration up to 1.55×10^{-4} M but leveled off at higher values. This behaviour has been treated according to Langmuir-Hishelwood kinetics. The activation energy was found to be 5.5 kJ/mol. The kinetics of photomineralization of 4-chlorophenol sensitised by Degussa P25 TiO_2 in O_2-saturated solution was studied by Mills and Morris (6). At pH 2 and $T = 30^\circ$C the initial relative rate of CO_2 photogeneration conforms to a Langmuir-Hinshelwood-type kinetic scheme. The overall activation energy for this photosystem was determined to be 16 ± 2 kJ/mol. Matthews (7) determined the rates of CO_2 formation from a number of common organic compounds, including phenol, 2-chlorophenol, 3-chlorophenol, and 4-chlorophenol. The dependence of their rates of oxidation obeys Langmuir-Hishelwood kinetics.

Recently, we have applied the photocatalytic reaction of TiO_2 to 1,3-dihydroxy-5-methoxybenzene (1,3-DHMB) which is from one class of organic contaminants: substituted phenols. The study examines the effects of initial concentration of 1,3-DHMB, pH of the medium, irradiation time, and temperature. A mechanism is proposed concerning the photocatalytic degradation route of 1,3-DHMB under the experimental conditions used.

2. METHODS

2.1. The Gas Recycling Reactor

All photodegradation experiments were performed in a gas recycling reactor. The reactor consists of a 36.2-cm-long

[1] Current address: Pacific Northwest National Lab, P.O. Box 999, MS K8-88, Richland, WA 99352. E-mail: marianne.sowa-resat@pnl.gov.

[2] To whom correspondence should be addressed. Fax: +90-212-287 2467. E-mail: yinel@boun.edu.tr.

0021-9517/01 $35.00

Pyrex tube with an inner diameter of 3.5 cm. To allow temperature regulation via water circulation, there is a sealed inner glass tube in the gas recycling reactor with a thickness of 2 cm. The TiO_2 suspension is contained in the annulus formed between the two tubes. The gas above the suspension is pumped using a Cole-Palmer peristaltic pump. A sintered glass disk, placed at the bottom of the reactor, provides circulation of air and prevents settlement of the suspension. All connections were made with Tygon tubing.

The reactor is located in an irradiation box (70 cm in length, 22 cm in width) containing six 20 W black light fluorescent lamps (General Electric F 20 T 12/BLB) that provide light of wavelength 320–440 nm. The lamps are positioned to surround the reaction vessel from three sides. Lamps can be lit individually as well as in conjunction with each other. The front side of the irradiation box was designed to operate as a door with the reactor attached. This maintains a uniform geometry throughout the experiments. A fan was placed at the top of the box and air was also continually circulated through the box in order to eliminate any heating effects of the lamps.

The incident photon flux for each lamp is measured using potassium ferrioxalate actinometry in the wavelength region (300–400 nm). However, TiO_2 particles are not capable of absorbing all the incident photon flux from a given source due to light scattering off the particle surface. Serpone (8) used the integrating sphere method to determine the fraction of light absorbed by Degussa P25 TiO_2. We follow Serpone's results by changing the TiO_2 loading from 0.1 to 4 g/L to estimate the fraction of light absorbed. For 1 g/L TiO_2 loading and for six lamps, the fraction of the absorption value was found as 0.489. This corresponds to an incident photon flux of 2.64×10^{-5} einstein $dm^{-3}\ s^{-1}$.

Since experiments are performed in a closed system (i.e., gas recycling reactor), the effect of relative humidity on the rate of degradation of 1,3-DHMB and on the rate of CO_2 formation is considered to be the same for each experiment. That is why concentration of water due to the mineralisation reaction of 1,3-DHMB is not determined in this study.

2.2. Reagents and Sample Preparation

Degussa P25 grade titanium dioxide was used as the photocatalyst. The average particle size was 30 nm. The BET surface area was $50 \pm 15\ m^2/g$. X-ray diffraction data have confirmed that TiO_2 is predominantly in the anatase form.

1,3-DHMB was from Fluka Chemical and used without further purification. Singly distilled water was deionized and used for the preparation of all solution. Stock solutions of 1,3-DHMB are prepared as 0.5 mol m^{-3} at the natural pH (pH 5.4). A catalyst concentration of 1 g/L of TiO_2 and a 144 mL min^{-1} of flow rate of air were used for all experiments unless otherwise stated. Prior to the photodegradation experiments, the suspension (containing 200 mL of the substrate and 1 g/L of TiO_2) was stirred for 30 min in the dark to achieve an adsorption equilibrium for the substrate on the photocatalyst. Solutions were always kept in the dark in order to prevent any interference from ambient light prior to irradiation. The pH values of the reaction solutions were adjusted by adding NaOH or $HClO_4$.

2.3. Analysis

The amount of CO_2 produced during reactions was determined with a Shimadzu (Gow Mac) gas chromatograph equipped with a thermal conductivity detector and a Porapak N column. Helium was used as a carrier gas at a flow rate of 60 mL min^{-1}. Calibrations were carried out using measured volumes of CO_2 added to the gas phase loop under identical conditions with the experiments. Sampling was made from the top of the reactor on which a mini inert valve is attached.

Following photodegradation, the concentration of substrate remaining was analysed by high-performance liquid chromatography (HPLC, CECIL 1100 series), using a CE 1100 liquid chromatography pump with CE 1220 variable wavelength monitor and a UV detector. The stationary phase was a Hypersil ODS column (particle size 10 μm). The mobile phase was a methanol : water (50 : 50) mixture. The measurements were performed at $\lambda = 274$ nm. All samples were filtered using Millipore films (0.45 μm) before injection.

3. RESULTS AND DISCUSSION

3.1. Effect of 1,3-DHMB Concentration

Photocatalytic degradation of 1,3-DHMB ($C_7H_6O(OH)_2$) is examined according to mineralisation reaction [1] and under two sets of experimental conditions:

$$C_7H_6O(OH)_2 + 15/2O_2 \rightarrow 7CO_2 + 4H_2O. \qquad [1]$$

The first set of experiments monitors the decrease in the initial concentration of 1,3-DHMB, in a concentration range of 0.5 to 2.0 mol m^{-3} (Fig. 1). The linearity in the inset of Fig. 1 indicates the kinetics of 1,3-DHMB degradation are zero order. Numerical results of apparent zero-order rate constants and rates are given in Table 1. As the initial concentration of 1,3-DHMB increases, the reaction rate becomes

TABLE 1

Kinetic Data for 1,3-DHMB Degradation

[1,3-DHMB] (mol m^{-3})	k' (s^{-1})	$R_{[1,3\text{-DHMB}]}$ (s^{-1})
2.0	0.056	0.056
1.0	0.063	0.063
0.7	0.037	0.037
0.5	0.048	0.048

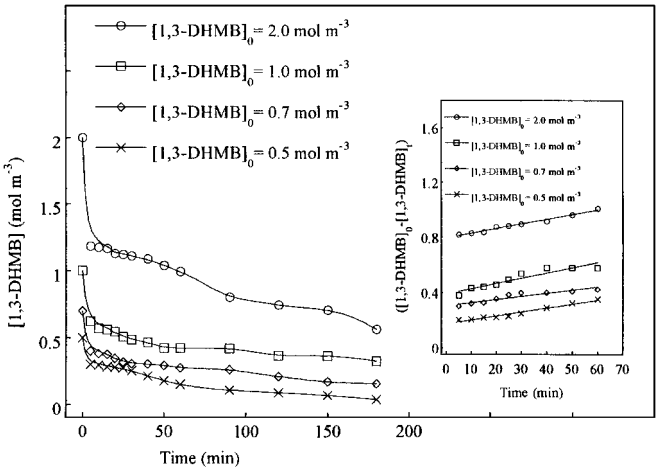

FIG. 1. Effect of change of 1,3-DHMB concentration on the degradation of 1,3-DHMB. Different concentration regions are marked on the graph. Inset: ($[1,3\text{-DHMB}]_0 - [1,3\text{-DHMB}]_t$) versus irradiation time. Conditions: $[TiO_2] = 1$ g/L, flow rate = 144 ml min^{-1}, pH 5.4, $T = 298$ K, $I_0 = 2.64 \times 10^{-5}$ einstein dm^{-3} s^{-1}.

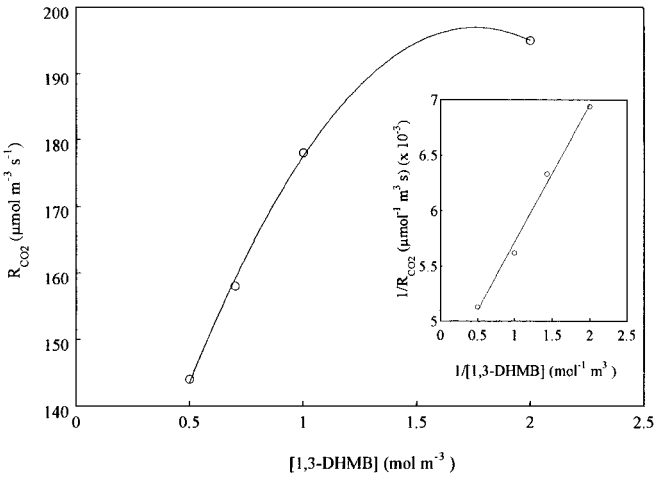

FIG. 3. Rate of CO_2 production versus 1,3-DHMB concentration. Inset: $1/R_{CO_2}$ as a function of 1/[1,3-DHMB]. Conditions: $[TiO_2] = 1$ g/L, pH 5.4, flow rate = 144 ml min^{-1}, $T = 298$ K, $I_0 = 2.64 \times 10^{-5}$ einstein dm^{-3} s^{-1}.

constant due to reaching the limit of available surface sites for species to be adsorbed on the TiO_2 surface.

The second set of experiments (Fig. 2) monitors the evolution of CO_2 in the 0.5–2.0 mol m^{-3} concentration range. When the rate of CO_2 production versus 1,3-DHMB concentration is plotted (Fig. 3, Table 2), a sharp increase is observed for initial concentrations ranging from 0.5 to 1.0 mol m^{-3}, but for 2.0 mol m^{-3} 1,3-DHMB solution, a plateau is observed in the rate of CO_2 evolution. From the linearity in the inset of Fig. 3, the reaction rate constant, k, is found to be 217 μmol m^{-3} s^{-1} and the adsorption constant, K, is found to be 4.22 m^{-3} mol^{-1}.

Both increasing the irradiation period from 60 min to 180 min and decreasing the initial 1,3-DHMB concentration have been found to increase the percentage degradation (Table 3). The lowest percentages are obtained with the highest concentration, 2.0 mol m^{-3}. This can be explained by the formation of some intermediates throughout the degradation process of 1,3-DHMB which could not easily be mineralised to CO_2. By decreasing the initial concentration of 1,3-DHMB, the percentages increase due to the presence of lower concentrations of intermediates which may subsequently degrade in the time scale of the experiment. By increasing the irradiation time, the percentages again increase, demonstrating the mineralisation of intermediates which occurs if the experiment is allowed to continue. However, complete degradation cannot be achieved for any concentration studied without exceeding 180 min irradiation.

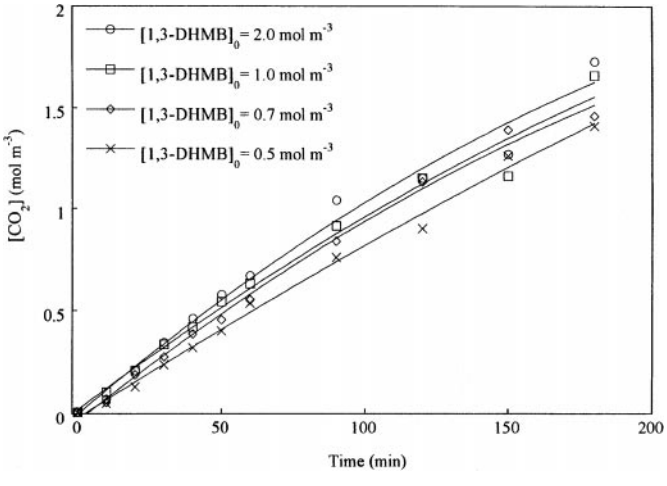

FIG. 2. Effect of initial 1,3-DHMB concentration on the concentration of CO_2 evolved as a function of irradition time. Conditions: $[TiO_2] =$ 1 g/L, flow rate = 144 ml min^{-1}, pH 5.4, $T = 298$ K, $I_0 = 2.64 \times 10^{-5}$ einstein dm^{-3} s^{-1}.

3.2. *Effect of pH*

A series of experiments have been performed to look at the effect of pH on the degradation of 1,3-DHMB and evolution of CO_2. The first set of experiments controls the pH of 1,3-DHMB/TiO_2 suspensions before and after irradiation (Table 4).

With the addition of TiO_2, the pH of suspensions, pH_1, changes due to the point of zero charge (pzc) value of TiO_2

TABLE 2

Effect of 1,3-DHMB Concentration on the Rate of Formation of CO_2

[1,3-DHMB] (mol m^{-3})	R_{CO_2} (μmol m^{-3} s^{-1})	1/[1,3-DHMB] (m^3 mol^{-1})	$1/R_{CO_2}$ (m^3 s^1 μmol^{-1})
2.0	195	0.5	5.13
1.0	178	1.0	5.62
0.7	158	1.43	6.33
0.5	144	2.0	6.94

TABLE 3

Degradation Percentage of 1,3-DHMB and Percentage Formation of CO_2

[1,3-DHMB] (mol m^3)	Degradation percentage of 1,3-DHMB		Percentage formation of CO_2	
	In 60 min	In 180 min	In 60 min	In 180 min
2.0	50	72	4.8	12
1.0	58	68	9.0	28
0.7	61	78	11	30
0.5	70	93	15	40

(4.7). The pzc value has been determined by measuring the changes of pH that occur when TiO_2 is added to water at different initial pH values. Since pH 3.5 is lower than pzc of TiO_2, no change is observed in the corresponding pH of 3.5. After irradiation, a noticeable decrease is observed due to the consumption of OH^- ions during photocatalytic degradation except for pH 3.5. Since dissociation of 1,3-DHMB (Eq. [2]) is inhibited in acidic media (i.e., dissociation shifts to the left) the amount adsorbed on the TiO_2 surface decreases, resulting in no change in the pH_2 value.

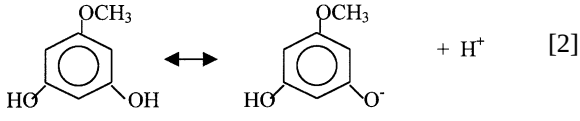

[2]

Table 5 gives the results of the second set of experiments in which the degradation of 1,3-DHMB is followed under irradiation in both the absence and the presence of TiO_2. In the absence of TiO_2, the decomposition times were found to fluctuate as pH increases, but for pH's 3.5, 5.4, and 11.0, no decrease in the concentration of 1,3-DHMB remaining in solution was found for irradiation times less than 25 min. Upon addition of TiO_2 the corresponding amount of 1,3-DHMB remaining in solution was found to decrease, indicating the favorable role of the photocatalyst in the degradation. The competition between OH^- ions and 1,3-DHMB ions for surface sites on the photocatalyst decreases the rate of degradation at pH 11.0. Figure 4 compares the

TABLE 4

Resulting pH Changes before (pH_1) and after Irradiation (pH_2) for 1,3-DHMB/TiO_2 Suspensions

pH	pH_1	pH_2	$\Delta pH = pH - pH_2$
3.5	3.5	3.5	0
5.2	4.5	4.2	1.2
7.0	6.3	4.3	2.7
9.0	8.9	5.3	3.7
11.0	10.8	10.7	0.3

TABLE 5

Effect of pH on the Degradation of 1,3-DHMB in the Absence and in the Presence of TiO_2

	$[1,3\text{-DHMB}]_0 = 0.5$ mol m^{-3}							
	pH 3.5		pH 5.4		pH 9.0		pH 11.0	
Time (min)	Without TiO_2	With TiO_2	Without TiO_2	With TiO_2	Without TiO_2	With TiO_2	Without TiO_2	With TiO_2
0	0.50	0.50	0.50	0.50	0.50	0.50	0.50	0.50
5	0.50	0.35	0.50	0.30	0.50	0.16	0.50	0.35
10	0.50	0.28	0.50	0.29	0.50	0.16	0.50	0.28
15	0.50	0.28	0.50	0.28	0.41	0.07	0.50	0.21
20	0.50	0.27	0.50	0.27	0.40	0.05	0.50	0.17
25	0.50	0.27	0.50	0.27	0.40	0.03	0.50	0.15
30	0.50	0.26	0.49	0.25	0.34	0.02	0.50	0.03
40	0.50	0.25	0.39	0.21	0.33	—	0.45	—
50	0.50	0.23	0.36	0.18	0.28	—	0.40	—
60	0.49	0.23	0.35	0.15	0.12	—	0.38	—

Note. Each numerical value represents the remaining 1,3-DHMB in the solution.

1,3-DHMB concentrations remaining in the solution in the absence and in the presence of TiO_2 at different pH values. The lowest amount remaining in solution corresponds to pH 9.0 in the presence and in the absence of TiO_2.

The last set of experiments monitors the formation of CO_2 at different pH values. A linear increase in the production of CO_2 is observed for 60 min irradiation (Fig. 5). Figure 5 inset shows the rate of CO_2 evolution as a function of pH. The highest rate is obtained at pH 9.0 (Table 6). The effect of pH on the formation of CO_2 and the degradation of 1,3-DHMB are shown together in Fig. 6 after 30 min irradiation time. The lowest concentration of 1,3-DHMB and the highest concentration of CO_2 are both obtained at pH 9.0, indicating this is the optimum pH for photocatalysis under the experimental conditions used.

3.3. Effect of Irradiation Time

The effect of irradiation time is investigated for 0.5 mol m^{-3} of 1,3-DHMB. Figure 7 gives the results of the percentage of remaining 1,3-DHMB in solution and the percentage formation of CO_2. Extending the irradiation time to

TABLE 6

Rate of Formation as a Function of pH for 40 min Irradiation Time

R_{CO_2} (μmol m^{-3} s^{-1})	pH
119	3.5
144	5.4
164	7.0
173	9.0

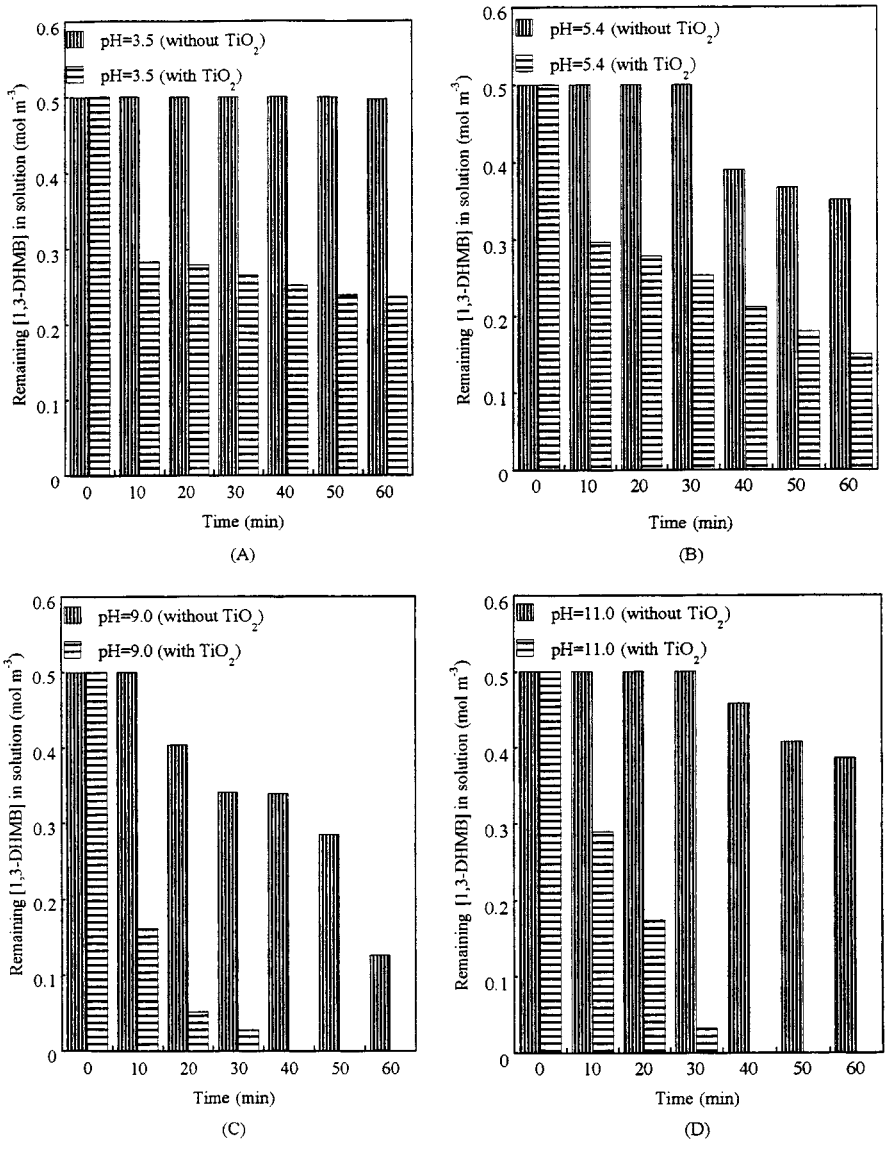

FIG. 4. Remaining [1,3-DHB] in solution in the absence and in the presence of TiO_2. (A) pH 3.5, (B) pH 5.4, (C) pH 9.0, (D) pH 11.0.

180 min decreases the percentage of remaining 1,3-DHMB, i.e., increases the degradation rate and also increases the percentage of CO_2 production.

3.4. *Effect of Temperature*

The formation of CO_2 is also investigated in the temperature range 298–333 K for 60 min irradiation time (Fig. 8). From the Arrhenius-type plot (Fig. 8 inset, Table 7), the apparent activation energy is calculated as 17.1 kJ/mol.

3.5. *Postulated Mechanism: Route of Oxidation*

In order to ascertain the route of oxidation for 1,3-DHMB ($C_7H_6O(OH)_2$), i.e., oxidation with photogenerated holes or reaction with $^{\cdot}OH$ radicals, the following mechanisms are assumed.

$$TiO_2 + h\nu \rightarrow h^+ + e^- \quad I \qquad [3]$$

$$h^+ + e^- \rightarrow \text{heat} \quad k_1[h^+] \qquad [4]$$

$$O_2 + e^- \rightarrow O_2^- \quad k_2[O_2][e^-] \qquad [5]$$

$$OH^- + h^+ \rightarrow {}^{\cdot}OH \quad k_3[OH^-][h^+] \qquad [6]$$

$$C_7H_6O(OH)_2 + h^+ \rightarrow\rightarrow CO_2 + H_2O$$

$$k_4[C_7H_6O(OH)_2][h^+] \qquad [7]$$

I is the rate of the light absorption by TiO_2 particles; k_1, k_2, k_3, and k_4 are the rate constants of the corresponding processes; and $[e^-]$ is included in k_1. If a steady-state condition

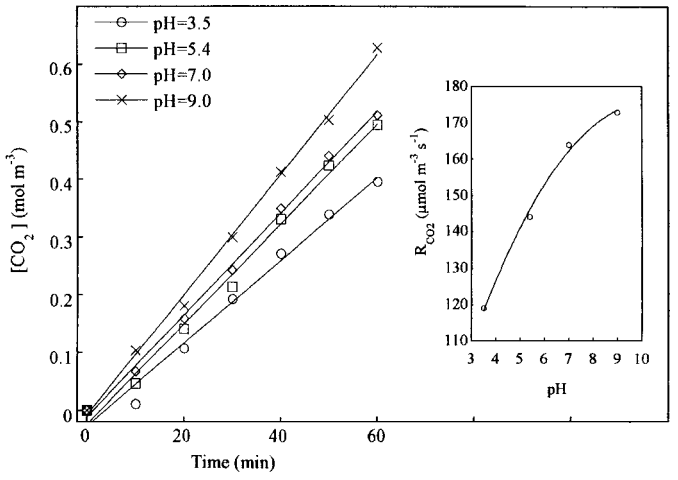

FIG. 5. Effect of pH on the concentration of CO_2 produced. Inset: R_{CO_2} as a function of pH. Conditions: $[TiO_2] = 1$ g/L, flow rate = 144 ml min^{-1}, $[1,3\text{-DHMB}]_0 = 0.5$ mol m^{-3}, $T = 298$ K, $I_0 = 2.64 \times 10^{-5}$ einstein dm^{-3} s^{-1}.

is assumed, i.e., the rate of photon arrival is equal to the rate of electron and hole consumption, then

$$I = (k_1 + k_3[\mathrm{OH}^-] + k_4[\mathrm{C_7H_6O(OH)_2}])[h^+] = k_2[\mathrm{O_2}][e^-]. \quad [8]$$

At this point, if it is assumed that $C_7H_6O(OH)_2$ oxidation is the rate determining step, then the initial rate of the process, R_i, may be expressed as $R_i = k_4[C_7H_6O(OH)_2][h^+]$. Assuming that rate of electron-hole recombination is very low

$$R_i = \frac{k_4[\mathrm{C_7H_6O(OH)_2}]I}{k_1 + k_3[\mathrm{OH}] + k_4[\mathrm{C_7H_6O(OH)_2}]} \quad [9]$$

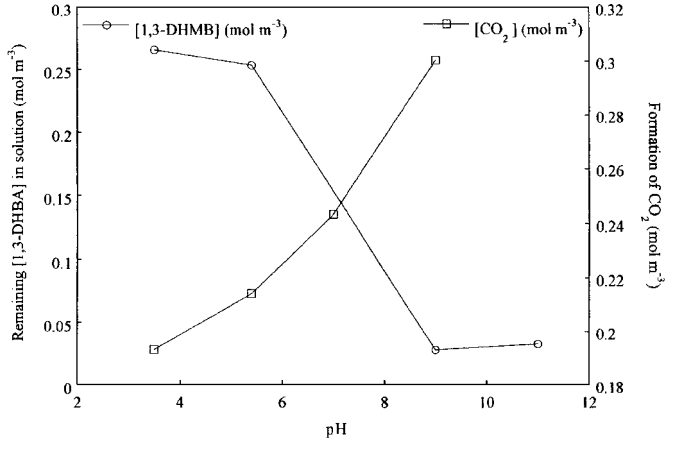

FIG. 6. Concentration of CO_2 produced and remaining 1,3-DHMB in solution as a function of pH after 30 min irradiation. Conditions: $[TiO_2] =$ 1 g/L, flow rate = 144 ml min^{-1}, $[1,3\text{-DHMB}]_0 = 0.5$ mol m^{-3}, $T = 298$ K, $I_0 = 2.64 \times 10^{-5}$ einstein dm^{-3} s^{-1}.

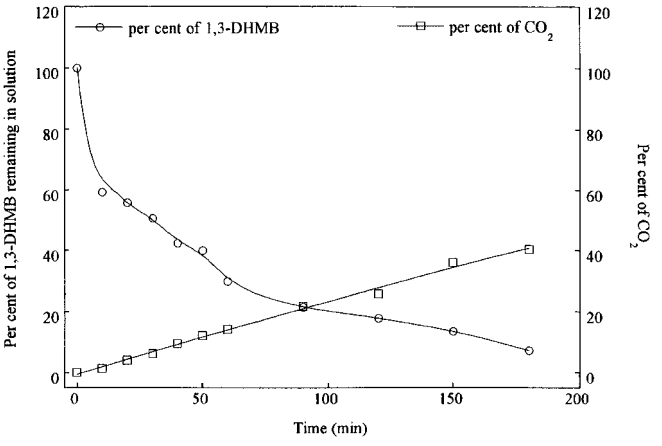

FIG. 7. The percentage of 1,3-DHMB remaining in solution and the percentage of CO_2 formation as a function of irradiation time. Conditions: $[TiO_2] = 1$ g/L, flow rate = 144 ml min^{-1}, pH 5.4, $[1,3\text{-DHMB}]_0 = 0.5$ mol m^{-3}, $T = 298$ K, $I_0 = 2.64 \times 10^{-5}$ einstein dm^{-3} s^{-1}.

compared to the rate of 1,3-DHMB oxidation and ·OH radicals formation, then

$$R_i = \frac{k_4[\mathrm{C_7H_6O(OH)_2}]I}{k_3[\mathrm{OH}] + k_4[\mathrm{C_7H_6O(OH)_2}]} \quad [10]$$

and rearranging

$$\frac{1}{R_i} = \frac{k_3[\mathrm{OH}]}{k_4[\mathrm{I}]} \frac{1}{[\mathrm{C_7H_6O(OH)_2}]} + \frac{1}{I}. \quad [11]$$

According to Eq. [11], when the reciprocal of the initial rate of CO_2 formation ($1/R_{CO_2}$) versus $1/[C_7H_6O(OH)_2]$ is plotted (Fig. 3 inset), a straight line is obtained whose slope (0.076) is equal to the value of $k_3[\mathrm{OH}]/k_4 I$. The rate of photon flux, I_0, is used as 2.64×10^{-5} einstein dm^{-3} s^{-1}.

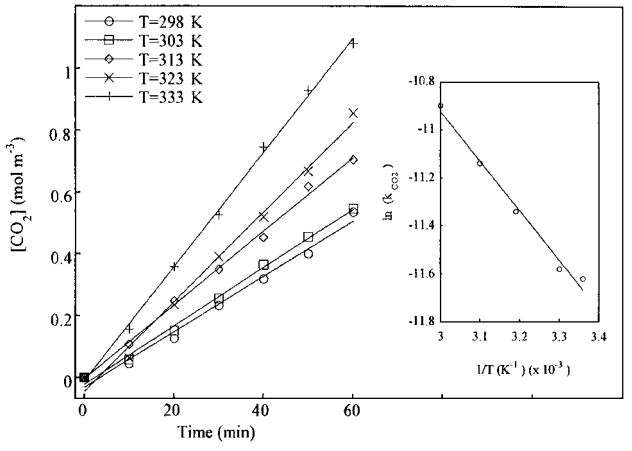

FIG. 8. Effect of temperature on the concentration of CO_2 produced. Inset: Arrhenius plot. Conditions: $[TiO_2] = 1$ g/L, flow rate = 144 ml min^{-1}, pH 5.4, $[1,3\text{-DHMB}]_0 = 0.5$ mol m^{-3}, $I_0 = 2.64 \times 10^{-5}$ einstein dm^{-3} s^{-1}.

TABLE 7

Arrhenius Data for 30 min Irradiation Time

$\ln(k_{CO_2})$	$1/T\ (\times 10^{-3})$
−11.65	3.355
−11.57	3.300
−11.34	3.195
−11.14	3.096
−10.89	3.003

Considering the natural pH (pH 5.4) of 1,3-DHMB, a ratio of $k_3/k_4 = 1.91 \times 10^5$ is deduced. Thus, the formation of ·OH radicals plays a more important role compared to the photogenerated holes for the oxidation of 1,3-DHMB.

4. CONCLUSION

In this study, we have investigated the photocatalytic degradation of 1,3-DHMB by monitoring the decrease in 1,3-DHMB and the resulting increase in the amount of formation of CO_2. Zero-order kinetics is found for the degradation of 1,3-DHMB. The Langmuir-Hinshelwood model holds for the formation of CO_2. The maximum degradation rate of 1,3-DHMB and the maximum formation rate of CO_2 are both obtained at pH 9.0. Activation energy is found to be 17.1 kJ/mol in the range of 298–333 K. Considering the rate of CO_2 formation, incident photon flux, pH of the reaction media, and initial concentration of 1,3-DHMB, the formation of ·OH radicals is found to be accountable for the photocatalytic degradation route of 1,3-DHMB.

ACKNOWLEDGMENT

This research was supported by the AVICENNE Research Programme of the European Community (Project No: 074).

REFERENCES

1. Okamoto, K., Yamamoto, Y., Tanaka, H., and Itaya, A., *Bull. Chem. Soc. Jpn.* **58**, 2023 (1985).
2. Matthews, R. W., and McEvoy, S. R., *J. Photochem. Photobiol. A.* **64**, 231 (1992).
3. Wei, T. Y., and Wan, C. C., *Ind. Eng. Chem. Res.* **30**, 1293 (1991).
4. Trillas, M., Pujol, M., and Domenech, X., *J. Chem. Technol. Biotechnol.* **55**, 85 (1992).
5. Al-Sayyed, G., D'Oliveria, J. C., and Pichat, P., *J. Photochem. Photobiol. A.* **58**, 99 (1991).
6. Mills, A., and Morris, S., *J. Photochem. Photobiol. A.* **71**, 75 (1993).
7. Matthews, R. W., *Wat. Res.* **24**, 653 (1990).
8. Serpone, N., *J. Adv. Oxid. Technol.* **2**, 203 (1997).